Carcinogenesis vol.34 no.9 pp.1968–1975, 2013
doi:10.1093/carcin/bgt147
Advance Access publication April 30, 2013

Polyunsaturated fatty acids affect the localization and signaling of PIP3/AKT in prostate cancer cells

Zhennan Gu[1,2], Jiansheng Wu[2], Shihua Wang[2], Janel Suburu[2], Haiqin Chen[1], Michael J.Thomas[3], Lihong Shi[2], Iris J.Edwards[4], Isabelle M.Berquin[2] and Yong Q.Chen[1,2,*]

[1]State Key Laboratory of Food Science and Technology, School of Food Science and Technology, Jiangnan University, Wuxi 214122, China and [2]Department of Cancer Biology, [3]Department of Biochemistry and [4]Department of Pathology, Wake Forest University School of Medicine, Winston-Salem, NC 27157, USA

*To whom correspondence should be addressed. Department of Cancer Biology, Wake Forest University School of Medicine, Medical Center Boulevard, Winston-Salem, NC 27157, USA. Tel: +1 336 713 7655; Fax: +1 336 713 7660;
Email: yqchen@wakehealth.edu

AKT is a serine–threonine protein kinase that plays important roles in cell growth, proliferation and apoptosis. It is activated after binding to phosphatidylinositol phosphates (PIPs) with phosphate groups at positions 3,4 and 3,4,5 on the inositol ring. In spite of extensive research on AKT, one aspect has been largely overlooked, namely the role of the fatty acid chains on PIPs. PIPs are phospholipids composed of a glycerol backbone with fatty acids at the *sn*-1 and *sn*-2 position and inositol at the *sn*-3 position. Here, we show that polyunsaturated fatty acids (PUFAs) modify phospholipid content. Docosahexaenoic acid (DHA), an ω3 PUFA, can replace the fatty acid at the *sn*-2 position of the glycerol backbone, thereby changing the species of phospholipids. DHA also inhibits AKT^{T308} but not AKT^{S473} phosphorylation, alters $PI(3,4,5)P_3$ (PIP_3) and phospho-AKT^{S473} protein localization, decreases $pPDPK1^{S241}$-AKT and AKT–BAD interaction and suppresses prostate tumor growth. Our study highlights a potential novel mechanism of cancer inhibition by ω3 PUFA through alteration of PIP_3 and AKT localization and affecting the AKT signaling pathway.

Introduction

Cardiovascular disease, cancer, obesity and type 2 diabetes collectively are responsible for more than 70% of disease-related mortality in the United States, and dietary fat plays critical roles in these illnesses. In cardiovascular disease, cholesterol is considered one of the major culprits, and in obesity, it is believed that a high-fat diet is partly responsible. However, how dietary fat contributes to cancer is less clear. Some fats are detrimental, whereas others may be beneficial to cancer patients.

Unlike the majority of known kinases that phosphorylate proteins, phosphoinositide-3-kinase (PI3K) is a lipid kinase that phosphorylates the third position hydroxyl group on the inositol ring of phosphatidylinositol (PI), generating phosphatidylinositol phosphate (PIP) (1). Dephosphorylation of PIP_3 is achieved by the action of phosphatase and tensin homolog (PTEN), a PI-3-phosphatase opposing PI3K action (2,3). Mutation in the *PIK3CA* gene, encoding the p110α PI3K catalytic subunit, was first reported in colon cancer (4), and an increasing number of mutations are being identified in human cancers (http://www.sanger.ac.uk/genetics/CGP/cosmic/). *PTEN* is one of the most frequently inactivated tumor-suppressor genes in human cancer (5,6). Thus, the PI3K/PTEN/AKT pathway is unique in which each gene is frequently mutated or amplified, is an integrator of lipid signaling from multiple inputs and is involved in almost every type of human cancer (7,8).

AKT is a serine–threonine protein kinase that plays important roles in cell growth, proliferation and apoptosis (9). Although it is well documented that AKT activation requires the binding of $PI(3,4)P_2$ and $PI(3,4,5)P_3$ (10–12), it is unclear whether fatty acids on the PIPs can affect their ability to activate AKT.

For several decades, epidemiological studies have reported effects of dietary fat on cancer risk (13–15). ω3 and ω6 polyunsaturated fatty acids (PUFAs) differentially impact cancer development and multiple molecular targets have been described (16–18). Despite extensive investigative efforts, mechanisms underlying these effects are still poorly understood. AKT inhibition by ω3 PUFA in cancer cells has been observed by us (19) and others (20–22). Because AKT activity is regulated by PIPs, we investigated the potential mechanism of dietary PUFA effect on phospholipid and AKT activity.

Abbreviations: AA, arachidonic acid; DHA, docosahexaenoic acid; EGFP, enhanced green fluorescent protein; EPA, eicosapentaenoic acid; FBS, fetal bovine serum; LA, linoleic acid; PA, palmitic acid; PC, phosphatidylcholine; PE, phosphatidylethanolamine; PI, phosphatidylinositol; PIP, phosphatidylinositol phosphate; PI3K, phosphoinositide-3-kinase; PS, phosphatidylserine; PTEN, phosphatase and tensin homolog; PUFA, polyunsaturated fatty acid.

Materials and methods

Cells

PC3 and LNCaP cells were purchased from the American Type Culture Collection (Manassas, VA). C4-2 and C4-2 transfected with BAD expression vector (C4-2BAD) cells were generously provided by Dr G.Kulik (Wake Forest School of Medicine). These cells were maintained in RPMI 1640 with 10% fetal bovine serum (FBS) and kept at 5% CO_2, 37°C. *Pten*-null mouse prostate epithelia cells were generated as described previously (23) and maintained in advanced Dulbecco's modified Eagle's medium (DMEM; Invitrogen, Carlsbad, CA) supplemented with 1% FBS.

Fatty acid treatment

PUFAs linoleic acid (LA, 18:2*n*-6), arachidonic acid (AA, 20:4*n*-6), eicosapentaenoic acid (EPA, 20:5*n*-3) and docosahexaenoic acid (DHA, 22:6*n*-3) were purchased from Nu-Chek Prep (Elysian, MN). For fatty acid treatment, cells were cultured in media containing 60 µM fatty acid conjugated with bovine serum albumin (fatty acid:albumin ratio of 4:1).

Total fatty acid and phospholipid measurement

Methods were as described previously (24).

PIP measurement

For PIP and PIP_2 analyses, *Pten*-null mouse prostate epithelial cells were starved in DMEM containing 60 µM fatty acids for 24 h and then in advanced DMEM with 1% FBS for 20 min at 37°C. For PIP_3 analysis, cells were starved in DMEM containing 60 µM fatty acids for 24 h and then stimulated by adding insulin (10 µg/ml) or ionomycin (10 µM) for indicated times at 37°C. Cells were rinsed with ice-cold PBS and directly lysed with a mixture of methanol and chloroform (2:1 ratio).

Quantitative measurement of phosphatidylinositol 3,4,5-trisphosphate followed the method of Guillou *et al.* (25). Briefly, internal standards were added, 200 ng each of dipalmitoyl-PIP_1, -PIP_2 and -PIP_3 (di-16:0-GPInsP1, di-16:0-GPInsP2 and di-16:0-GPInsP3) followed by 725 µl of chloroform containing carrier lipids (4 ng/µl each of cholesterol, phosphatidylcholine (PC), and phosphatidylethanolamine (PE) and 1 ng/µL each of PI and phosphatidic acid) and 170 µl of water containing 2M HCl and 10 mM tetrabutylammonium hydrogen sulfate. Preliminary studies had demonstrated that di-16:0-GPInsP1, di-16:0-GPInsP2 and di-16:0-GPInsP3 were not present in the experimental samples. Further steps of lipid extraction were carried out as described by Guillou *et al.* (25) except that the synthetic upper and lower phases were prepared without the use of tetrabutylammonium hydrogen sulfate. Sample transfer steps used silanized glass Pasteur pipettes. Washed lipid extracts were transferred to 1.5 ml polytetrafluoroethylene microfuge tubes and evaporated under a stream of argon. Samples were evaporated to near dryness, redissolved in 50 µl of HPLC solvent B (acetonitrile:chloroform:methanol:water at 30:30:32:8 with 20 mM ethylamine) and transferred to silanized glass autosampler vials. Samples were analyzed on the day of lipid extraction. Gradient conditions were as described by Pettit *et al.* (26,27).

Separations were carried out on an Agilent 1100 HPLC controlled by Xcalibur™ software, using a modification of the method of Pettit *et al.* (26,27). Before each injection, the needle and injector loop were washed with 5–100 µl

injections of solvent B containing 500 µM tetrabutylammonium hydrogen sulfate. Samples (10 µl) were injected onto a 1 × 150 mm Phenomenex Luna Silica2 normal-phase column packed with 3 µm diameter particles. Components were eluted at a constant flow rate of 100 µl/min using the following gradient profile: 100% solvent A (chloroform:methanol:water at 90:9.5:5 with 20 mM ethylamine) for 2 min, 45% solvent B over 1 min, 60% solvent B over 4 min, hold for 5 min, 100% solvent B over 1 min, hold for 10 min and then regenerate the column at 100% solvent A for 26 min.

The eluant was analyzed using a Thermo Finnigan TSQ Quantum Discovery Max triple-quadrupole mass spectrometer with an electrospray ion source. Typical source parameters were as follows: spray potential −3400 V, sheath gas 20, ion sweep gas 1.5, skimmer offset 7 V and ion-transfer capillary temperature 360°C. Data were acquired in centroid mode with a 0.5 s scan time. For full scan liquid chromatography–mass spectrometry experiments, spectra were acquired from m/z 887–1500. Selected ion monitoring experiments used a window of 1 m/z with a dwell time of 100 ms. Liquid chromatography–tandem mass spectrometry experiments used argon collision gas at 0.8 or 1.0 mTorr. A collision energy of 35 eV was found to be optimal for neutral loss of 98 Da and for polar head group product ions (m/z 321 for PIP1, 401 for PIP2 and 481 for PIP3). Higher collision energy (55 eV) more efficiently yielded fatty acyl anions as products.

Western blotting

Prostate tissues and cells were lysed in a buffer [50 mM Tris–HCl pH 7.5, 150 mM NaCl, 1% Triton X-100, 1 mM dithiothreitol, 1× protease inhibitor cocktail and 1× phosphatase inhibitor cocktail (Roche Applied Science, Indianapolis, IN)]. Western blotting was performed as described previously (24) with anti-pAKT^{S473}, anti-pAKT^{T308}, antitotal AKT, antitotal PDPK1, anti-pPDK1^{S241} (Cell Signaling Technology, Danvers, MA), antitotal BAD (Millipore, Billerica, MA), as well as anti-β-actin (Sigma–Aldrich, St Louis, MO). Images were taken using FluorChem E Digital Darkroom and quantified using software AlphaView SA (Alpha Innotech, San Leandro, CA).

Immunoprecipitation

C4-2 and C4-2BAD cells were first cultured in Advanced DMEM with 1% FBS and 60 µM fatty acid AA or DHA at 37°C for 48 h. Cells were then lysed with RIPA buffer [150 mM NaCl, 1% NP-40, 0.5% deoxycholate, 50 mM Tris–HCl (pH 7.5), 1× protease Inhibitor cocktail and 1× phosphatase inhibitor cocktail (Roche Applied Science)] on ice for 30 min. Cell lysates were then centrifuged at 10 000 r.p.m. at 4°C for 15 min. Supernatants were collected and antitotal AKT (Millipore), antitotal PDPK1 (BD Biosciences) or antitotal BAD (Millipore) was added at the concentration suggested by manufacturers. The samples were then rotated at 4°C for 1 h. Prewashed Protein-G Mag Sepharose Xtra beads (GE Healthcare Biosciences, Piscataway, NJ) were added into the sample at a ratio of 15:1 (sample volume:bead volume). The samples were rotated for 1 h at 4°C. The sample beads were then washed three times with lysis buffer and boiled in sodium dodecyl sulfate–polyacrylamide gel electrophoresis sample buffer for 5 min. The samples were then analyzed by western blotting.

Immunocytochemistry

Cells grown on poly-L-lysine-coated coverslips were fixed with 2% paraformaldehyde and permeabilized with 0.2% saponin/1% bovine serum albumin. Freshly dissected prostate tissues were fixed in 3.7% paraformaldehyde and 50% glycerol–PBS (pH 7) at −20°C overnight. Fixed tissues were rinsed with PBS and mounted with optimal cutting temperature compound and kept at −80°C. Three micrometer sections were cut in a cryostat. Immunostaining was performed using anti-PI(3,4,5)P_3 antibody (Echelon Biosciences, Salt Lake City, UT) according to the manufacturer's instructions. Pictures were taken under a fluorescent microscope.

Immunofluorescence microscopy

LNCaP cells were transduced with lentivirus expressing enhanced green fluorescent protein (EGFP) or PH_{BTK} domain-EGFP fusion proteins. Cells were cultured on poly-D-lysine-treated coverslips for 16 h in culture medium containing 60 µM AA or DHA, followed by incubation with 10 µM of LY294002 for 15 min. Cells were then washed with ice-cold culture medium and stimulated with culture medium for 5 min at 37°C. Cells were fixed and examined under a fluorescent microscope. For PIP3 stimulation experiment, cells were cultured on poly-D-lysine-treated coverslips for 16 h in culture medium, and then washed and replaced with serum-free DMEM for 24 h. Cells were then stimulated with 5 µM of PIPs for 20 min at 37°C. Cells were fixed and examined under a fluorescent microscope.

Immunohistochemistry

Phospho-AKT staining was performed by incubation with an antiphospho-AKT^{S473} antibody (Cell Signaling Technology), followed by a biotinylated antirabbit secondary antibody and streptavidin alkaline phosphatase (Super Sensitive Link-Label IHC Detection Systems; BioGenex) as described (24), visualized with Vector Red Substrate (SK-5100; Vector Laboratories) and counterstained with hematoxylin.

Diet

Diets were prepared by the custom animal diet laboratory of the Animal Resources Program at Wake Forest University. All diets contained 397 kcal/100 g, and 30% of energy was from fat, 50% from carbohydrates and 30% from proteins. The ω6/ω3 ratio was 1 in the ω3 diet and 40 in ω6 diet (24).

Transgenic mice

Prostate-specific *Pten*-knockout and fat1 transgenic mice were generated as described previously (24). Protocol for studies that involved animals was approved by the Institutional Animal Care and Use Committee of Wake Forest University. *Bad* knockout mice were kindly provided by Dr G.Kulik (Wake Forest School of Medicine).

Statistical analysis

Quantitative data with two groups were tested by unpaired Student's *t*-test using Excel software (Microsoft, Seattle, WA). Quantitative data of more than two groups were initially evaluated by analysis of variance followed by Bonferroni–Holm test using Excel software with Daniel's XL ToolBox add-in (http://xltoolbox.sourceforge.net/index.html). $P < 0.05$ was considered significant.

Results

Phospholipid content is modified by PUFAs

ω3 and ω6 PUFAs are essential fatty acids. Mammals can neither synthesize them *de novo* nor interconvert ω6 to ω3 or *vice versa*; therefore, these PUFAs must be acquired from diet. Vegetable oils are abundant in ω6 PUFAs such as LA (18:2*n*-6) and AA (20:4*n*-6), whereas fish oil is a rich source of ω3 PUFAs in the form of EPA

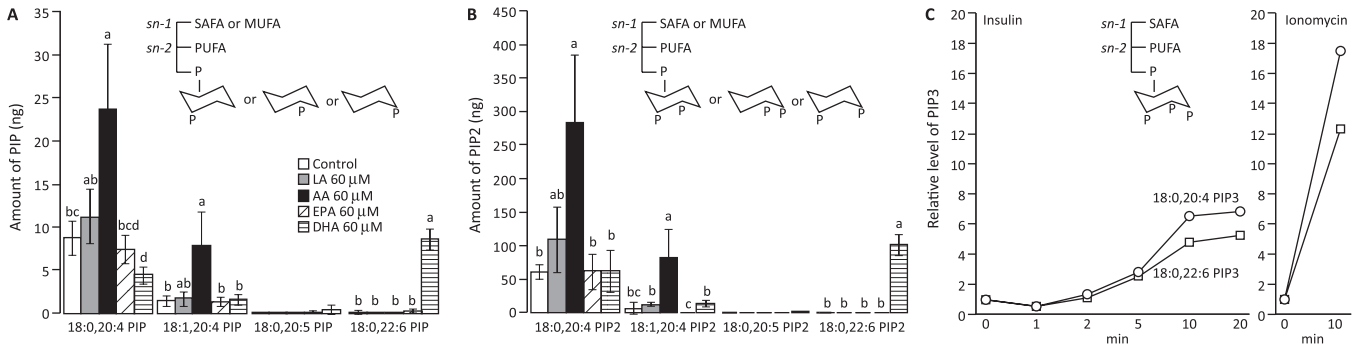

Fig. 1. PUFAs modify the structure of PIP. Mouse *Pten*-null cells (3×10^6) were incubated in media with 60 µM fatty acids (LA, AA, EPA, DHA or vehicle control) for 24 h and then with media plus 1% FBS for 20 min. (**A**) PIP levels, including PI(3)P, PI(4)P and PI(5)P. (**B**) PIP_2 levels, including PI(3,4)P_2, PI(3,5)P_2 and PI(4,5)P_2. Three independent experiments were performed. Averages and standard deviations are shown. Bars labeled with different letters are significantly different from each other (analysis of variance, $P < 0.05$). (**C**) Relative level of PIP_3. Cells grown in medium containing AA (circles) or DHA (squares) for 24 h were stimulated with insulin (10 µg/ml) or ionomycin (10 µM) for the indicated times at 37°C.

(20:5*n*-3) and DHA (22:6*n*-3) (17). To assess the uptake, PC3 prostate tumor cells were treated with 30–60 µM of fatty acids, concentrations below 100–5000 µM levels found in human plasma (28). ω6 PUFAs (LA, 18:2*n*-6; AA, 20:4*n*-6) or ω3 PUFAs (EPA, 20:5*n*-3; DHA, 22:6*n*-3) were quantified by fatty acid methyl ester analysis. By comparing the input to the increased amount of PUFA in treated cells measured by fatty acid methyl ester analysis, we estimated that approximately 25% of input PUFAs were incorporated into cells within 48 h. LA treatment resulted in significant increases in cellular LA and AA, whereas AA treatment only increased the level of AA. EPA treatment resulted in significantly higher level of EPA, docosapentaenoic acid (22:5*n*-3) and a small amount of DHA, whereas DHA treatment significantly increased cellular level of DHA, docosapentaenoic acid and EPA (Supplementary Figure S1, available at *Carcinogenesis* Online). These data indicate that cells can efficiently take up PUFAs, and there is conversion from LA to AA but little retroconversion from AA to LA, and there are both forward and retroconversions among ω3 PUFAs.

In mammals, phospholipids generally have a saturated fatty acid at the *sn*-1 position and an unsaturated fatty acid at the *sn*-2 position of the glycerol backbone (29–31). To determine the effect of PUFA on phospholipid structure, PC3 cells were treated with LA, AA, EPA or DHA, followed by analysis of PC, phosphatidylserine (PS), PE and PI. Many phospholipid species were detectable, with myristic acid (14:0), palmitic acid (PA, 16:0), palmitoleic acid (POA, 16:1), stearic acid (18:0), oleic acid (18:1) or eicosanoic acid (20:0) at the *sn*-1 position in combination with PA, POA, stearic acid, oleic acid, LA, AA, EPA or DHA at the *sn*-2 position. PUFA treatment significantly altered the proportion of PC, PS, PE and PI species containing the corresponding fatty acid (Supplementary Figures S2–S5, available at *Carcinogenesis* Online). Therefore, phospholipids synthesized by tumor cells are subject to modification by PUFA.

PC, PS, PE and PI are components of cell membranes and also involved in cell signaling. PI can be phosphorylated to form PIPs that regulate the function of proteins containing the pleckstrin homology domain, such as AKT. To investigate whether PUFA can affect AKT function, mouse *Pten*-null prostate cells were treated with LA, AA, EPA or DHA and PIP profiles were determined. Treatment with AA (20:4*n*-6) or DHA (22:6*n*-3) for 24 h resulted in significant increases in the relative amount of respective monophosphate PIPs 18:0;20:4PIP, 18:1;20:4PIP, 18:0;22:6PIP (Figure 1A) and bisphosphate PIPs 18:0;20:4PIP$_2$, 18:1;20:4PIP$_2$, 18:0;22:6PIP$_2$ (Figure 1B). Treatment with LA or EPA did not substantially change the levels of PIPs

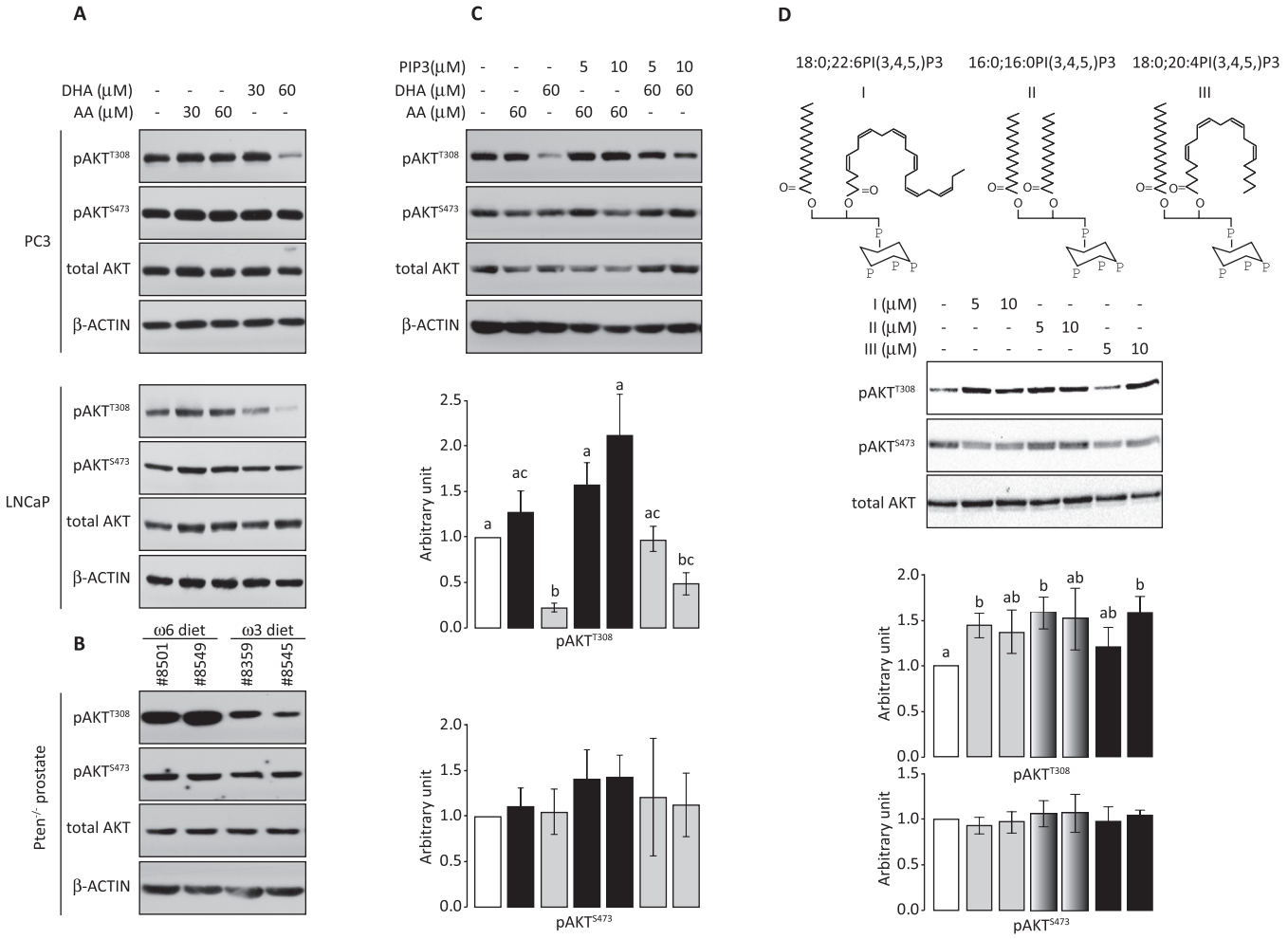

Fig. 2. ω3 PUFA inhibits AKT^{T308}, but not AKT^{S473}, phosphorylation. (**A**) Western blot analysis of phosphorylated AKT in PC3 and LNCaP cells treated with the indicated amount of AA or DHA. (**B**) Levels of phosphorylated AKT in mouse prostates from prostate-specific *Pten*-null mice on ω6 or ω3 diets. (**C**) PC3 cells were first treated with DHA and then incubated with the indicated amount of 18:0;20:4PI(3,4,5)P$_3$ for 20 min. Phospho-AKT level was normalized by total AKT. The normalized value in untreated sample was set at one arbitrary unit. Three independent experiments were performed. Relative arbitrary units of pAKT^{T308} and pAKT^{S473} and standard deviations are shown. (**D**) PC3 cells were starved for 24 h and stimulated with the indicated amount of 18:0;22:6PI(3,4,5)P$_3$, 16:0;16:0PI(3,4,5)P$_3$ or 18:0;20:4PI(3,4,5)P$_3$ (structures shown at the top) for 20 min. Western blot was performed as described above. Three independent experiments were performed. Relative arbitrary units of pAKT^{T308} and pAKT^{S473} and standard deviations are shown. Bars labeled with different letters are significantly different from each other (analysis of variance, $P < 0.05$).

containing corresponding fatty acids (Figure 1A and B). The levels of PIP_3 were too low to be reliably detected under the same culture conditions. To determine whether both AA- and DHA-containing PIP_2 can be efficiently converted to PIP_3, cells were incubated with AA or DHA for 24 h and stimulated with insulin for up to 20 min. The level of AA-containing PIP_3 (18:0;20:4PIP_3) increased in AA-treated cells, and the level of DHA-containing PIP_3 (18:0;22:6PIP_3) increased in DHA-treated cells after insulin stimulation (Figure 1C). PIP_3 level could also be increased by calcium ionophore (Figure 1C). Both insulin and calcium ionophore ionomycin provoke rapid changes in the production of PIP_3 (32,33).

AKT^{T308} phosphorylation is inhibited by ω3 PUFAs

We showed previously that *n*–3 PUFA reduced phosphorylation of the downstream AKT target BAD and induced BAD-dependent tumor cell apoptosis *in vivo* and *in vitro* (24). Activation of AKT requires phosphorylation at the threonine 308 and serine 473 residues. To confirm the role of PIP_2 and PIP_3 in the activation of AKT, cells were starved for 12 h to lower the basal level of active AKT, followed by incubation with 5 μM of PI(3,4)P_2 or PI(3,4,5)P_3 for 20 min. Incubation with PI(3,4)P_2 increased $pAKT^{S473}$, and incubation with PI(3,4,5)P_3 increased $pAKT^{T308}$ (Supplementary Figure S6A, available at *Carcinogenesis* Online), which is consistent with previous reports (11,12).

Because AKT activity is regulated by PIPs and PIP composition is influenced by fatty acid, we tested whether AA and DHA have different effects on AKT activation. FBS is rich in ω6 PUFAs, including AA and LA (34) and the content of ω6 PUFAs in FBS varies from batch to batch. To minimize these uncontrollable factors, we added known concentration of ω6 PUFA (AA) to the medium containing minimum amount of serum (1%) as our control. PC3 and LNCaP prostate cancer cells were treated with 30 or 60 μM of AA or DHA for 48 h and the levels of $pAKT^{T308}$ and $pAKT^{S473}$ were assessed. DHA treatment reduced $pAKT^{T308}$ but not $pAKT^{S473}$ (Figure 2A). AA treatment had no significant effect on AKT phosphorylation in these cells (Figure 2A). To validate this observation *in vivo*, prostate-specific *Pten* knockout mice were fed ω3- or ω6-PUFA diet for 3 months. As mentioned previously, both ω6 and ω3 PUFAs are essential lipids necessary for health. All animal diets contain variable amounts of these fatty acids. Therefore, it is important to define an appropriate control diet. We used an ω6 diet, which is based on a typical American diet consisting of an ω6 to ω3 ratio of 40:1 and 30% energy from fat, as control. An isocaloric ω3 diet, which has an ω6 to ω3 ratio of 1:1, was used as an experimental diet. Prostates were dissected and evaluated for AKT activation. Compared to the ω6-PUFA diet, the ω3-PUFA diet reduced $pAKT^{T308}$ but not $pAKT^{S473}$ (Figure 2B). Thus, both *in vitro* and *in vivo* results indicate that DHA inhibits AKT^{T308} phosphorylation.

Because AKT^{T308} phosphorylation is regulated by PIP_3, we determined whether the DHA-induced reduction in $pAKT^{T308}$ can be overcome by AA-containing PIP_3. PC3 cells were treated with 60 μM DHA for 48 h followed by a 20 min incubation with 18:0;20:4PI(3,4,5)P_3. Incubation of DHA-treated cells with the AA-containing PIP_3 enhanced AKT^{T308} phosphorylation but had little effect on AKT^{S473} phosphorylation (Figure 2C), indicating that 18:0;20:4PI(3,4,5)P_3 could partially reverse the inhibitory effect of DHA on AKT^{T308} phosphorylation. Experiments were also performed with 16:0;16:0PI(3,4,5)P_3, and similarly, the PA-containing PIP_3 could partially reverse the DHA inhibitory effect. Thus, it is possible that DHA-treated cells synthesize DHA-containing PIP_3, which is less capable of stimulating AKT^{T308} phosphorylation compared with AA- or PA-containing PIP_3.

PA-, AA- and DHA-containing PI(3,4,5)P_3 can similarly stimulate AKT^{T308} phosphorylation

PA is a 16-carbon saturated fatty acid, AA is a 20-carbon fatty acid with four double bonds and DHA is a 22-carbon fatty acid with six double bonds. Compared with PA and AA, DHA has a longer carbon chain and higher degree of unsaturation, which could alter the ability of DHA-containing PIP_3 to facilitate PDPK1-mediated phosphorylation of AKT^{T308}. To address this possibility, we analyzed the phospho-AKT after PIP_3 incubation in culture as reported previously (10–12). PC3 cells were starved for 12 h to reduce the endogenous level of PIPs and incubated with 5 or 10 μM of 16:0;16:0PI(3,4,5)P_3, 18:0;20:4PI(3,4,5)P_3 or 18:0;22:6PI(3,4,5)P_3 for 20 min, cells were harvested and then AKT phosphorylation was determined. Results indicated that all three PIP_3 species increased AKT^{T308} but not AKT^{S473} phosphorylation (Figure 2D). This difference may be explained by the fact that exogenously delivered PI(3,4,5)P_3, unlike the endogenous PIP_3, must enter the cell through the plasma membrane, as indicated by the translocation of PH_{BTK}-EGFP protein (Figure 3), and thus can trigger phosphorylation of AKT^{T308} due to high concentration of PIP3 on cell membrane, regardless of its fatty acid composition.

DHA alters the localization of PI(3,4,5)P_3 and $pAKT^{S473}$ protein

Fatty acids on PIPs tether these molecules to cellular membranes. Fatty acid length and degree of unsaturation might affect PIP membrane targeting. Therefore, localization of the endogenous PIP_3 was determined by immunofluorescent microscopy using an antibody that is selective for PI(3,4,5)P_3 as reported (35) and confirmed by antibody–antigen competition immunofluorescent microscopy (Supplementary Figure S6B, available at *Carcinogenesis* Online). In PC3 and LNCaP cells treated with AA, PIP_3 was primarily localized on the plasma membrane. However, in cells treated with DHA, PIP_3 was mainly observed in the cytosol, perhaps in cytoplasmic vesicles (Figure 4A). To further confirm this observation, LNCaP cells were transfected with vectors expressing an EGFP or EGFP fused to the BTK pleckstrin homology domain, which binds to PIP_3 selectively

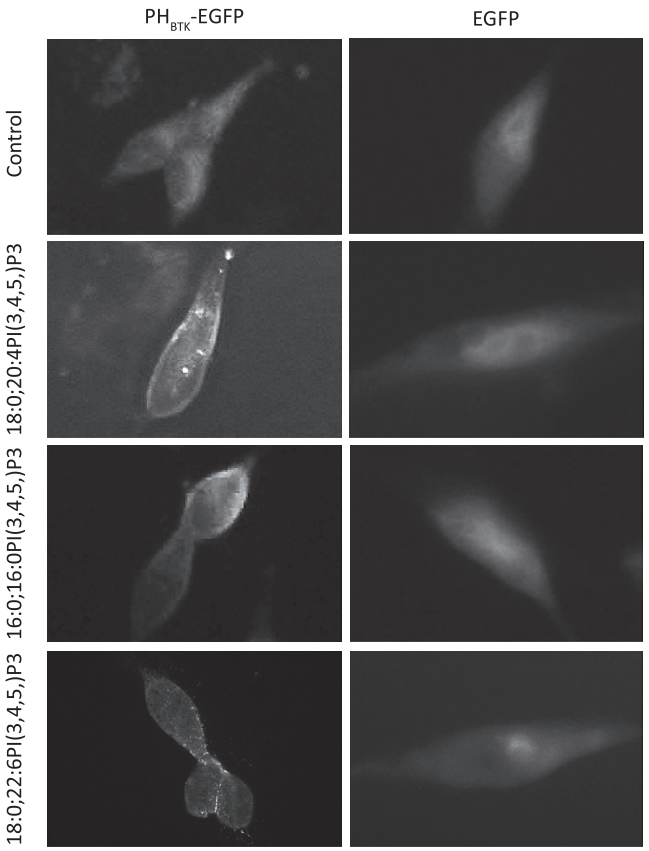

Fig. 3. Membrane translocation of PH_{BTK} domain-EGFP stimulated by exogenous PI(3,4,5)P_3. LNCaP cells were transduced with recombinant lentivirus expressing EGFP or PH_{BTK}-EGFP fusion protein. Cells were cultured in serum-free medium and stimulated with vehicle only, 5 μM 18:0;20:6PI(3,4,5)P_3, 16:0;16:0PI(3,4,5)P_3 or 18:8;20:4PI(3,4,5)P_3 for 20 min. Note all three PIP_3 stimulate translocation of PH_{BTK}-EGFP to plasma membrane.

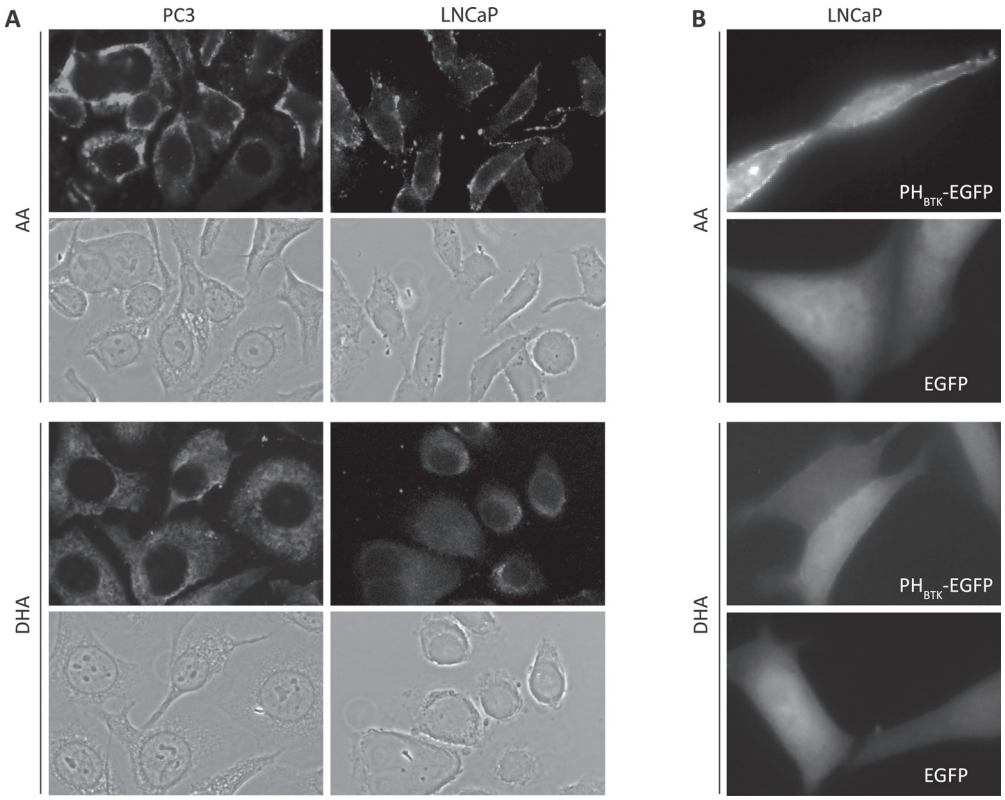

Fig. 4. PUFAs alter the localization of PI(3,4,5)P_3. (**A**) PC3 and LNCaP cells were cultured in medium supplemented with AA or DHA for 24 h, stimulated with media plus 1% FBS for 20 min and then stained with anti-PI(3,4,5)P_3 antibody. Bright color indicates the staining of PIP_3. (**B**) LNCaP cells, expressing EGFP or PH_{BTK}-EGFP fusion protein, were incubated with 60 μM AA or DHA overnight. Cells were stimulated with media containing 1% FBS and 60 μM AA or DHA.

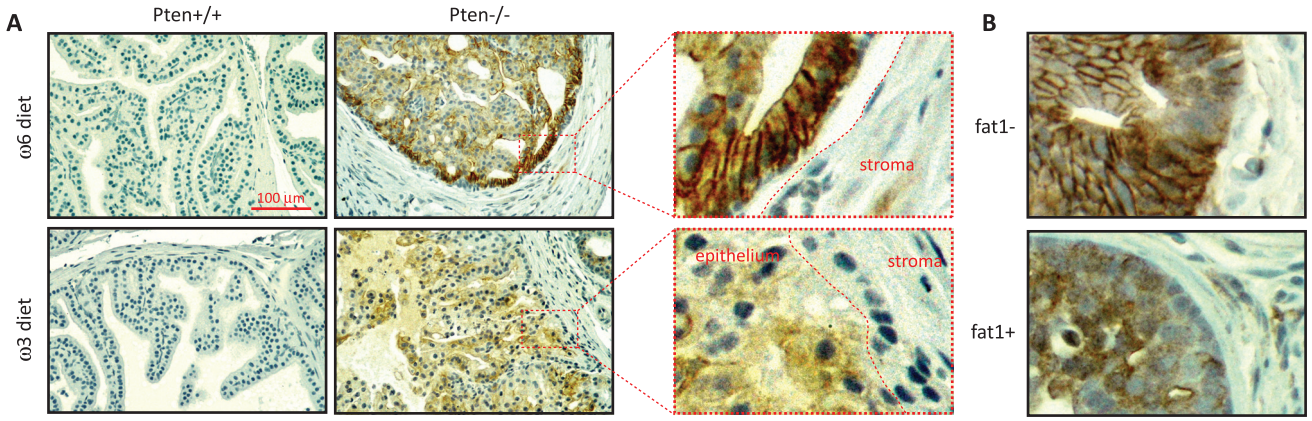

Fig. 5. PUFAs alter the localization of pAKT^{S473}. (**A**) Paraffin sections of *Pten* wild-type and null prostates from mice on ω3 and ω6 diets were stained with anti-pAKT^{S473}. (**B**) Paraffin sections of *Pten*-null prostate with or without the *fat1* gene (*fat1*^{T} or *fat1*$^-$) on the ω6 diet were stained with anti-pAKT^{S473}. Brown color indicates positive staining for pAKT^{S473}.

(36,37). PH_{BTK}-EGFP was detected on the plasma membrane of AA-treated, but not DHA-treated cells, whereas no such difference was seen regardless of treatment in EGFP-expressing cells (Figure 4B). These data suggest that ω3 PUFA treatment promotes localization of PI(3,4,5)P_3 away from the plasma membrane in tumor cells.

Because AA and DHA appear to affect PIP_3 localization differentially, they may also alter AKT protein localization. To test this possibility, distribution of pAKT^{S473} was determined by immunohistochemistry. pAKT^{S473} was used for the localization of phospho-AKT because AKT^{S473} phosphorylation is not affected by ω6 or ω3 diet (Figure 2). In prostate-specific *Pten*-knockout mice, the probasin promoter-driven Cre is activated by androgen and therefore *Pten* deletion occurs mainly in prostate epithelial cells. Like PIP_3, pAKT^{S473} was not detectable in *Pten* wild-type prostate tissues. In *Pten*-null mice, pAKT^{S473} was detected on the plasma membrane in the prostate from mice on ω6-PUFA control diet, but its distribution was largely diffuse throughout the epithelium in the prostate from mice on ω3-PUFA diet (Figure 5A). This difference in distribution is not due to a different level of the pAKT^{S473} protein, because approximately equal amounts of the protein were present in prostates from mice on either diet as reported previously (18) and shown in Figure 2B. To minimize potential confounding effects from other ingredients in the mouse diet, the *fat1* transgene, which converts ω6-PUFA to ω3-PUFA, was bred into the prostate-specific *Pten*-knockout genetic background. *Pten*-null mice with or without the *fat1* transgene (*fat1*^{T} and *fat1*$^-$) were fed the same ω6 diet. Similar to the data from the above experiment, the

pAKT^{S473} protein was concentrated on the plasma membrane in the prostate from *fat1*$^{-}$ mice; however, it was diffused throughout the epithelium in the prostate from *fat1*^{T} mice (Figure 5B). Thus, results obtained from both dietary and genetic models indicate that ω3 PUFA promotes cytoplasmic localization, whereas ω6 PUFA promotes plasma membrane localization of the pAKT^{S473} protein.

DHA reduces the interactions of PDPK1–AKT and AKT–BAD

AKT is phosphorylated at T308 by PDPK1 (38) and at S473 by mTORC2 (39) upon binding to PIPs. DHA inhibition of AKT^{T308}, but not AKT^{S473}, phosphorylation may be a result of diminished PDPK1–AKT interaction due to the altered PI(3,4,5)P_3 localization. C4-2 prostate tumor cells were treated with AA or DHA and the interaction between PDPK1 and AKT proteins was assayed by immunoprecipitation followed by western blotting. DHA treatment reduced pPDPK1^{S241}-AKT but not total PDPK1–AKT interaction (Figure 6A). Reduction in serine 241 phosphorylation of PDPK1 inhibits its activity (40) and consequently AKT^{T308} phosphorylation.

The proapoptotic protein BAD is an AKT substrate, and phosphorylation at S112 and S136 is inhibitory and therefore promotes survival. Previously, we have shown that ω3 PUFA treatment diminishes BAD phosphorylation (24). However, the molecular mechanism of reduced BAD phosphorylation was not determined. To assess this issue, tumor cells were treated with AA or DHA and the interaction between BAD and AKT protein was analyzed. DHA treatment, compared with AA, induced a significant reduction in BAD–AKT protein interaction (Figure 6B), which may trigger cell apoptosis. Interestingly, BAD-associated AKT was phosphorylated at S473 but not at T308 (Figure 6B).

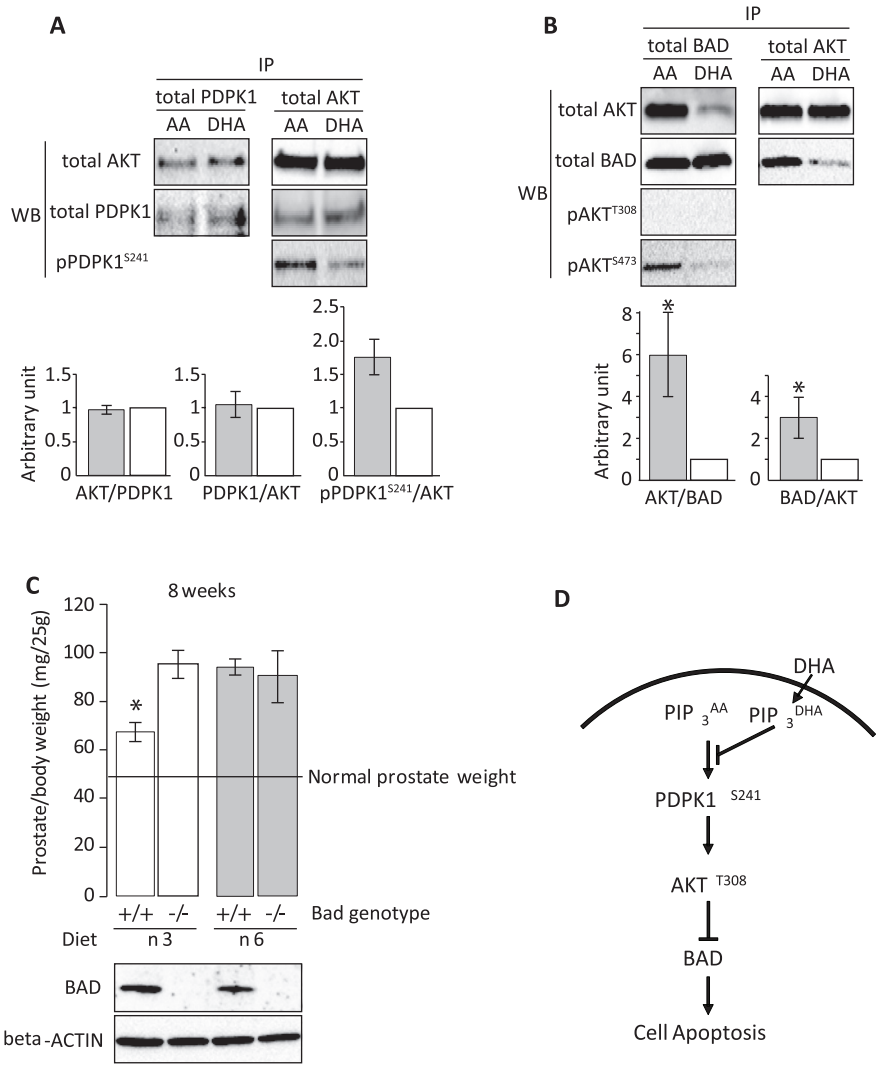

Fig. 6. PUFA influences the interactions of PDK1–AKT and AKT–BAD. (**A**) C4-2 cells were cultured in medium containing AA or DHA for 48 h. Protein extracts from these cells were immunoprecipitated with mouse anti-PDPK1 or anti-AKT. Western blot analyses were then performed with rabbit anti-AKT, anti-PDK1 and anti-pPDK1^{S241} antibodies. AKT level was normalized by total PDK1 in the IP-PDK/WB-AKT; PDK1 and pPDK1^{S241} levels were normalized by total AKT in the IP-AKT/WB-PDK experiment. Normalized levels in DHA-treated samples (white bars) were set at one arbitrary unit. Averages from three repeated experiments and standard deviations are shown. (**B**) C4-2 and C4-2 BAD cells were cultured in medium containing AA or DHA for 48 h. Immunoprecipitation was performed with mouse antihemagglutinin epitope (C4-2 BAD) or mouse anti-AKT (C4-2), followed by western blotting with rabbit anti-BAD, anti-AKT and anti-phospho-AKT antibodies. AKT level was normalized by total BAD in the IP-BAD/WB-AKT, and BAD level was normalized by total AKT in the IP-AKT/WB-BAD experiment. Normalized levels in DHA-treated samples (white bars) were set at one arbitrary unit. Averages from three repeated experiments and standard deviations are shown (* indicates $P < 0.05$, Student's *t*-test). (**C**) Knockout of *Bad* reduced the suppressive effects of ω3 PUFA on prostate cancer. *Pten*-null mice with or without *Bad* (*Pten*$^{-/-}$;*Bad*$^{+/+}$ and *Pten*$^{-/-}$;*Bad*$^{-/-}$) were fed with ω3 or ω6 diet for 8 weeks. Average mouse prostate weight (mg/25 g body weight, seven mice per group) and error bars are shown. BAD protein expression was confirmed by western blot. (**D**) Scheme of DHA action. Dietary DHA can be incorporated into *sn*-2 position of PIP_3 to form PIP_3^{DHA}. PIP_3^{DHA} will antagonize PIP_3^{AA} on cell membrane and induce BAD-associated cell apoptosis.

Knockdown of *BAD* in human PC3 and LNCaP cells could block ω3 PUFA-induced cell death (24). To validate the role of BAD in mediating tumor suppression by ω3 PUFA *in vivo*, *Bad* knockout mice were crossed with prostate-specific *Pten*-null mice. *Pten*$^{-/-}$;*Bad*$^{+/+}$ and *Pten*$^{-/-}$;*Bad*$^{-/-}$ male mice were fed ω6 control or ω3 diet. ω3 PUFA, compared with ω6 PUFA, reduced prostate tumor growth in the *Bad* wild-type background. However, knockout of *Bad* diminished the suppressive effect of ω3 PUFA on prostate tumor growth (Figure 6C). These results suggest that BAD protein is necessary for ω3-mediated suppression of prostate tumor growth in *Pten*-null mice and DHA-containing PIP_3 (PIP_3^{DHA}) could antagonize ω6 fatty acid-containing PIP_3 to induce BAD-associated cell apoptosis as illustrated in Figure 6D.

Discussion

Epidemiological data suggest that some fats are detrimental and others may be beneficial to cancer patients. However, how dietary fat modulates cancer is less clear. Our study provides a potential mechanistic link between PUFAs, phospholipid content and AKT signaling in prostate cancer cells. DHA replaces fatty acid at the *sn*-2 position of the glycerol backbone generating different species of phospholipids, inhibits AKT^{T308} but not AKT^{S473} phosphorylation, alters PIP_3 and phospho-AKT^{S473} localization, decreases AKT–BAD interaction and suppresses tumor growth.

In our study, cells were cultured in the presence of FBS and therefore had high levels of AA-containing 18:0;20:4PI (Supplementary Figure S5, available at *Carcinogenesis* Online). This may explain why AA treatment had minimal effect on AKT^{T308} phosphorylation despite an increase in AA-containing PI. In contrast, cells had low levels of DHA-containing 18:0;22:6PI and DHA treatment resulted in a significant increase in DHA-containing PI. Cells had a dose-dependent response to DHA treatment (Figure 2A).

AKT activation requires both T308 and S473 phosphorylation. Our results show that DHA treatment inhibits PDPK1 activity by translocating PIP3 and reducing its phosphorylation at S241 position and consequently reduces phosphorylation of AKT at T308. BAD is associated with $pAKT^{S473}$ but not $pAKT^{T308}$ (Figure 6B), suggesting that AKT protein can exist in only T308 or S473 phosphorylated form, and BAD may be phosphorylated by $pAKT^{S473}$. Although DHA treatment inhibits AKT^{T308} phosphorylation, as well as $pAKT^{S473}$–BAD interaction, disrupted $pAKT^{S473}$–BAD interaction may be mainly responsible for reduced BAD phosphorylation and thus enhanced apoptosis (24), and disrupted $pAKT^{S473}$ may contribute to the inhibition of other tumor-promoting pathways (41).

At present, it is unclear whether DHA at the *sn*-2 position of PIP_3 alone or the collective content changes of phospholipids is responsible for the cytoplasmic localization of PIP_3 and $pAKT^{S473}$. In the mammalian brain, a large amount of DHA is esterified to membrane phospholipids in the gray matter and neurons. There, unlike in cancer cells, DHA seems to activate AKT and protect neuron cells from apoptosis (42–44). Interestingly, the principal esterified PUFA at the *sn-2* position on PE and PS is DHA but that on PI is AA in the neuronal membranes (45–48). In contrast, DHA is the major PUFA esterified on PI (Supplementary Figure S5, available at *Carcinogenesis* Online) and PIPs (Figure 1) after supplementation in cancer cells. This difference in PI species may explain the opposite response of neuron and cancer cells to DHA and is supportive of the notion that AA- and DHA-containing PIP_3 differentially regulate AKT.

Supplementary material

Supplementary Figures 1–7 can be found at http://carcin.oxfordjournals.org/

Funding

National Institutes of Health (R01CA107668, P01CA106742, R01CA163273 to Y.Q.C.); American Institute for Cancer Research (07B087 to Y.Q.C.); North Carolina Biotechnology (2007-IDG-1021 to M.J.T.); National Institutes of Health Shared Instrumentation (1S10RR027940); National Cancer Institute (5P30CA12197).

Acknowledgements

We thank Dr Y.Hu for assistance in experiment and Dr W.Lands for reading the manuscript.

Conflict of Interest Statement: None declared.

References

1. Cantley,L.C. (2002) The phosphoinositide 3-kinase pathway. *Science*, **296**, 1655–1657.
2. Stokoe,D. (2001) PTEN. *Curr. Biol*., **11**, R502.
3. Comer,F.I. *et al.* (2002) PI 3-kinases and PTEN: how opposites chemoattract. *Cell*, **109**, 541–544.
4. Samuels,Y. *et al.* (2004) High frequency of mutations of the PIK3CA gene in human cancers. *Science*, **304**, 554.
5. Chalhoub,N. *et al.* (2009) PTEN and the PI3-kinase pathway in cancer. *Annu. Rev. Pathol*., **4**, 127–150.
6. Hollander,M.C. *et al.* (2011) PTEN loss in the continuum of common cancers, rare syndromes and mouse models. *Nat. Rev. Cancer*, **11**, 289–301.
7. Yuan,T.L. *et al.* (2008) PI3K pathway alterations in cancer: variations on a theme. *Oncogene*, **27**, 5497–5510.
8. Cully,M. *et al.* (2006) Beyond PTEN mutations: the PI3K pathway as an integrator of multiple inputs during tumorigenesis. *Nat. Rev. Cancer*, **6**, 184–192.
9. Manning,B.D. *et al.* (2007) AKT/PKB signaling: navigating downstream. *Cell*, **129**, 1261–1274.
10. Franke,T.F. *et al.* (1997) Direct regulation of the Akt proto-oncogene product by phosphatidylinositol-3,4-bisphosphate. *Science*, **275**, 665–668.
11. Scheid,M.P. *et al.* (2002) Phosphatidylinositol (3,4,5)P3 is essential but not sufficient for protein kinase B (PKB) activation; phosphatidylinositol (3,4) P2 is required for PKB phosphorylation at Ser-473: studies using cells from SH2-containing inositol-5-phosphatase knockout mice. *J. Biol. Chem*., **277**, 9027–9035.
12. Stokoe,D. *et al.* (1997) Dual role of phosphatidylinositol-3,4,5-trisphosphate in the activation of protein kinase B. *Science*, **277**, 567–570.
13. Willett,W. (1989) The search for the causes of breast and colon cancer. *Nature*, **338**, 389–394.
14. Lee,M.M. *et al.* (2000) Dietary fat and breast cancer. *Annu. Rev. Nutr*., **20**, 221–248.
15. Kolonel,L.N. (2001) Fat, meat, and prostate cancer. *Epidemiol. Rev*., **23**, 72–81.
16. Berquin,I.M. *et al.* (2011) Polyunsaturated fatty acid metabolism in prostate cancer. *Cancer Metastasis Rev*., **30**, 295–309.
17. Berquin,I.M. *et al.* (2008) Multi-targeted therapy of cancer by omega-3 fatty acids. *Cancer Lett*., **269**, 363–377.
18. Chen,Y.Q. *et al.* (2007) Dietary fat-gene interactions in cancer. *Cancer Metastasis Rev*., **26**, 535–551.
19. Hu,Y. *et al.* (2010) Syndecan-1-dependent suppression of PDK1/Akt/bad signaling by docosahexaenoic acid induces apoptosis in prostate cancer. *Neoplasia*, **12**, 826–836.
20. Schley,P.D. *et al.* (2005) Mechanisms of omega-3 fatty acid-induced growth inhibition in MDA-MB-231 human breast cancer cells. *Breast Cancer Res. Treat*., **92**, 187–195.
21. Friedrichs,W. *et al.* (2011) Omega-3 fatty acid inhibition of prostate cancer progression to hormone independence is associated with suppression of mTOR signaling and androgen receptor expression. *Nutr. Cancer*, **63**, 771–777.
22. Toit-Kohn,J.L. *et al.* (2009) Docosahexaenoic acid induces apoptosis in colorectal carcinoma cells by modulating the PI3 kinase and p38 MAPK pathways. *J. Nutr. Biochem*., **20**, 106–114.
23. Wang,S. *et al.* (2012) Effect of dietary polyunsaturated fatty acids on castration-resistant Pten-null prostate cancer. *Carcinogenesis*, **33**, 404–412.
24. Berquin,I.M. *et al.* (2007) Modulation of prostate cancer genetic risk by omega-3 and omega-6 fatty acids. *J. Clin. Invest*., **117**, 1866–1875.
25. Guillou,H. *et al.* (2007) Quantitative measurement of phosphatidylinositol 3,4,5-trisphosphate. *Methods Enzymol*., **434**, 117–130.
26. Pettitt,T.R. (2009) Lipidomic analysis of phospholipids and related structures by liquid chromatography-mass spectrometry. *Methods Mol. Biol*., **462**, 25–41.

27. Pettitt,T.R. *et al.* (2006) Analysis of intact phosphoinositides in biological samples. *J. Lipid Res*., **47**, 1588–1596.
28. Brodersen,R. *et al.* (1990) Multiple fatty acid binding to albumin in human blood plasma. *Eur. J. Biochem*., **189**, 343–349.
29. Soma,M.R. *et al.* (1992) Triglyceride metabolism in 3T3-L1 cells. An *in vivo* 13C NMR study. *J. Biol. Chem*., **267**, 11168–11175.
30. Bernhard,W. *et al.* (1995) Composition of phospholipid classes and phosphatidylcholine molecular species of gastric mucosa and mucus. *Biochim. Biophys. Acta*, **1255**, 99–104.
31. Beermann,C. *et al.* (2005) sn-position determination of phospholipid-linked fatty acids derived from erythrocytes by liquid chromatography electrospray ionization ion-trap mass spectrometry. *Lipids*, **40**, 211–218.
32. Blero,D. *et al.* (2001) The SH2 domain containing inositol 5-phosphatase SHIP2 controls phosphatidylinositol 3,4,5-trisphosphate levels in CHO-IR cells stimulated by insulin. *Biochem. Biophys. Res. Commun*., **282**, 839–843.
33. Ekinci,F.J. *et al.* (1999) Hyperactivation of mitogen-activated protein kinase increases phospho-tau immunoreactivity within human neuroblastoma: additive and synergistic influence of alteration of additional kinase activities. *Cell. Mol. Neurobiol*., **19**, 249–260.
34. Stoll,L.L. *et al.* (1984) Changes in serum influence the fatty acid composition of established cell lines. *In Vitro*, **20**, 732–738.
35. Chen,R. *et al.* (2002) A monoclonal antibody to visualize PtdIns(3,4,5)P(3) in cells. *J. Histochem. Cytochem*., **50**, 697–708.
36. Várnai,P. *et al.* (1999) Phosphatidylinositol 3-kinase-dependent membrane association of the Bruton's tyrosine kinase pleckstrin homology domain visualized in single living cells. *J. Biol. Chem*., **274**, 10983–10989.
37. Balla,T. *et al.* (2002) Visualizing cellular phosphoinositide pools with GFP-fused protein-modules. *Sci. STKE*, **2002**, pl3.
38. Stephens,L. *et al.* (1998) Protein kinase B kinases that mediate phosphatidylinositol 3,4,5-trisphosphate-dependent activation of protein kinase B. *Science*, **279**, 710–714.
39. Sarbassov,D.D. *et al.* (2005) Phosphorylation and regulation of Akt/PKB by the rictor-mTOR complex. *Science*, **307**, 1098–1101.
40. Casamayor,A. *et al.* (1999) Phosphorylation of Ser-241 is essential for the activity of 3-phosphoinositide-dependent protein kinase-1: identification of five sites of phosphorylation *in vivo*. *Biochem. J*., **342 (Pt 2)**, 287–292.
41. Hart,J.R. *et al.* (2011) Phosphorylation of AKT: a mutational analysis. *Oncotarget*, **2**, 467–476.
42. Akbar,M. *et al.* (2002) Protective effects of docosahexaenoic acid in staurosporine-induced apoptosis: involvement of phosphatidylinositol-3 kinase pathway. *J. Neurochem*., **82**, 655–665.
43. Akbar,M. *et al.* (2005) Docosahexaenoic acid: a positive modulator of Akt signaling in neuronal survival. *Proc. Natl Acad. Sci. USA*, **102**, 10858–10863.
44. Figueroa,J.D. *et al.* (2012) Docosahexaenoic acid pretreatment confers protection and functional improvements after acute spinal cord injury in adult rats. *J. Neurotrauma*, **29**, 551–566.
45. Breckenridge,W.C. *et al.* (1972) The lipid composition of adult rat brain synaptosomal plasma membranes. *Biochim. Biophys. Acta*, **266**, 695–707.
46. Sun,G.Y. *et al.* (1972) Phospholipids and acyl groups of synaptosomal and myelin membranes isolated from the cerebral cortex of squirrel monkey (Saimiri sciureus). *Biochim. Biophys. Acta*, **280**, 306–315.
47. Ikemoto,A. *et al.* (2000) Effect of n-3 fatty acid deficiency on fatty acid composition and metabolism of aminophospholipids in rat brain synaptosomes. *Lipids*, **35**, 1107–1115.
48. Glomset,J.A. (2006) Role of docosahexaenoic acid in neuronal plasma membranes. *Sci. STKE*, **2006**, pe6.

Received January 29, 2013; revised April 5, 2013; accepted April 26, 2013